Journal of Energy Storage 46 (2022) 103883

Contents lists available at ScienceDirect

Journal of Energy Storage

journal homepage: www.elsevier.com/locate/est

Research Papers

# Capturing curtailed renewable energy in electric power distribution networks via mobile battery storage fleet

Hedayat Saboori, Shahram Jadid *

*Electrical Engineering Department, Iran University of Science and Technology, Tehran, Iran*

ARTICLE INFO

*Keywords:*
Renewable energy
Curtailment recovery
Mobile battery storage fleet
Operation optimization
Distribution network

ABSTRACT

In this paper, a new scheduling model is proposed for the daily operation of a truck-mounted Mobile Battery Energy Storage Systems (MBES) fleet employed in a distribution network. The distribution network is installed with various wind and PV distributed resources wherein a portion of the renewable-based generation capacity is curtailed due to various technical reasons. The MBES fleet scheduling model aims at minimizing curtailed renewable energy by absorbing and releasing excess energy when and where needed. Accordingly, the variable spatial and temporal renewable generation curtailment is recovered by optimal spatio-temporal and power-energy scheduling of the MBES fleet. The required transportation time for the MBES unit transportation comprising detachment, movement, and attachment is considered efficiently. Besides, a detailed breakdown of the MBES transportation cost is presented and modelled via a new formulation. The proposed MBES fleet operation model can be easily integrated into the available commercial distribution optimal power flow packages. Considering linearity, the model can handle very large-scale real-life networks without convergence problems by achieving global optima. The model is numerically tested, and simulation results demonstrate its effectiveness for recovering a considerable share of the curtailed renewable energy irrespective of the resources type, generation time period, or installation location.

## 1. Introduction

Today, employing renewable energy resources has proven to be a sustainable solution to overcome fossil fuels' problems. The exhaustibility, environmental pollutions, high prices, and low energy security with these new resources are no longer insurmountable energy industry challenges [1,2]. The renewable energy industry has grown exponentially over the past decades, increasing its share in the energy portfolio. It has even progressed to the point where the system planners have triggered an energy system with 100% renewable resources [3].

However, with the steady growth of renewable energy penetration, a new challenge has emerged. Today, this field's problem, especially for regions with high renewable shares, is not the production capacity but the impossibility of consuming all the energy produced [4]. In other words, currently, a portion of the renewable generation capacity is forcibly cut off for various reasons despite access to extra free and clean generation ability [5]. This problem is especially the case in distribution networks, which have higher percentages of renewable sources and stringent technical constraints. Accordingly, in some time periods, especially during the peak periods of renewable production, despite load demand, part of the produced renewable energy is inevitably cut, and the rest of the load is supplied from the utility grid (upstream substation) [6]. This forced reduction in the amount of renewable production, namely curtailment, in turn, increases the daily operating costs (energy purchase cost) and substations and feeders loading, reduces the network capacity to cope with higher demand growth, and most importantly, increases air pollution due to the carbon footprint of grid electricity [7]. The renewable energy curtailment may occur because of an over-generation condition due to demand and/or renewable potential forecasting errors. The market and contracts mechanism and limitations are other causes of renewable energy curtailment. The technical limitation in absorbing and distributing generated energy is the main reason for renewable curtailment in distribution networks. These limitations appear mainly as bus overvoltage and/or feeder overload at time periods with abundant renewable generation [8].

There are two leading solutions to recover curtailed renewable energy. The first one is to convert excess energy into other materials. The converted material may be used in other industries, stored for later use,

* Corresponding author.
*E-mail addresses:* h_saboori@elec.iust.ac.ir (H. Saboori), jadid@iust.ac.ir (S. Jadid).

https://doi.org/10.1016/j.est.2021.103883
Received 13 April 2021; Received in revised form 16 December 2021; Accepted 19 December 2021
Available online 30 December 2021

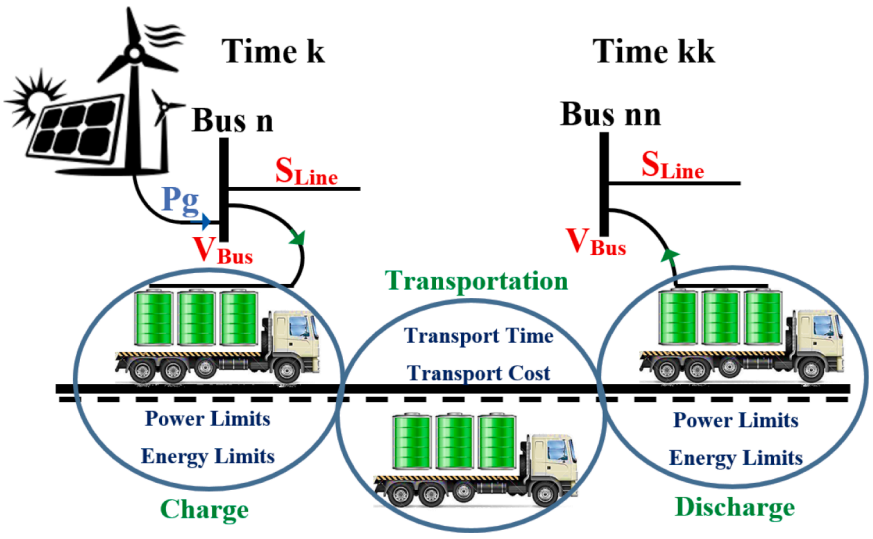


**Fig. 1.** Application of mobile battery for renewable curtailment mitigation.

or converted back into electrical energy [9]. These methods are known as power-to-x solutions, and the most important of them are power-to-gas (hydrogen) and power-to-liquid (ammonia) [10,11]. The other solution is to store an amount of curtailed renewable energy to be used later when needed [12]. Currently, the renewable energy is stored mainly using stationary electrochemical battery energy storage systems [13,14]. The stationary batteries used for this purpose can also be deployed for other applications at the end of the life of the batteries [15]. The problem with this solution is the temporal-spatial variation of curtailed renewable energy. Due to the battery's fixed location, it is not possible to absorb and store a high percentage of curtailed renewable energy. This problem is a result of flowing charging power between the battery and renewable plant installation location. In other words, the two main problems of bus overvoltage and feeder overload also remain. Accordingly, the stationary battery can only reduce renewable curtailment due to over-generation, relatively rare in the distribution networks. The solution to this problem is to absorb the excess renewable energy at its production and time. In other words, the storage device must be capable of variable temporal and spatial utilization. This feature can be achieved by moving stationary batteries [16].

A Mobile Battery Energy Storage (MBES) system is a set of storage cells and required power electronic converter compacted and containerized to be movable. The whole battery system can be transported by train or truck. The truck-mounted battery containers are the most popular system in the distribution networks because of higher flexibility in transportation medium and parking location, resulting in more network candidates for connection [17]. Application of the truck-mounted MBES for enhancing distribution network resiliency at emergency and disaster event has evaluated previously in [18–21]. The optimal sitting of a stationary battery system [22] will be converted to the spatio-temporal location optimization for the mobile counterpart owning to the dynamical changes in the battery location. This is one of the most important differences between stationary and mobile battery systems. Network reconfiguration has been always one of the effective solutions to the distribution network operation challenges [23]. The mobile battery can act as a virtual reconfiguration scheme in the distribution networks with low reconfiguration opportunities. However, the mobile battery application to recover renewable energy curtailment in distribution networks is not addressed technically yet. Some other solutions to the renewable energy curtailment have been proposed and developed especially for the transmission networks, namely Dynamic Thermal Rating (DTR) [24,25]. Considering the spatial and temporal variation of the produce renewable energy, the MBES can efficiently recover curtailed energy if scheduled optimally. This application is aimed at this paper by proposing a novel operation schedule model for a fleet of MBES units. The MBESs are employed in a distribution network with multiple renewable distributed resources in the form of wind turbines and PV panels.

The proposed operation model aims to recover the curtailed renewable energy as much as possible by defining the optimal spatio-temporal and power-energy schedule of each MBES unit. To do this, novel formulations have been proposed for modelling and considering transportation time, including detachment, movement, and attachment of the MBES to the network buses. Besides, a detailed breakdown and new modelling of MBES transportation cost are presented. The presented model is linear in objective function and constraints and can be easily used for real-life, very large-scale systems without convergence and optimality problems. The scheduling's ultimate goal is to recover curtailed energy from PV and wind resources as much as possible, having the lowest daily operation cost. Concisely, the novelty of this paper can be listed as:

- Proposing a new operation schedule model for an MBES fleet considering the required time for transportation and detailed analysis and modelling of transportation cost.
- Proposing a linear model capable of handling very large-scale real-life networks.
- Minimizing renewable energy curtailment irrespective of the resources type, generation time period, or installation location.

The paper excluding this introductory part is organized as follows. The concept and application of the MBES to recover curtailed renewable energy and governing rules are described in Section 3. The proposed mathematical model for MBES fleet operation is the context of a distribution network is outlined in Section 4. The numerical test of the model, along with the inputs and parameters, are shown in Section 5. Sections 6 and 7 presents simulation results for the conventional network without MBES fleet and employing them and the comparisons and discussions. Finally, Section 8 offers concluding remarks of the paper.

## 2. Application of mobile battery for curtailment recovery

Fig. 1 depicts a generic bus of a distribution network installed with renewable energy resources. The Pg shows the total power produced by these resources at a typical time period. At least three factors influence the acceptance level of this value by the network. The first one is the power balance in the network. Summation over all generated power and consumed power has to be the same at any time period. Thus, the grid

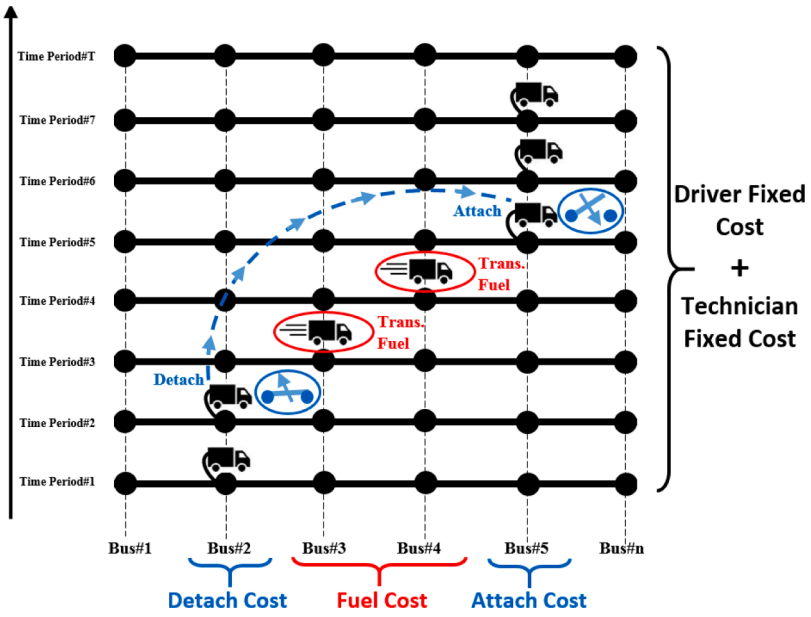


**Fig. 2.** General rules of MBES transportation and connection.

will be able to absorb renewable energy from all distributed generation resources up to its maximum load. The extra amount will be forcibly cut because it will not be transferable to the next hours. The second limitation in accepting the generated power is the allowable amplitude of the bus overvoltage. Increasing the amount of power injected by renewable sources in the bus will only be possible by increasing the bus voltage. This increase to the standard level (usually 5%) is acceptable. Injection of the generated power causes the voltage to rise more than this amount will be cut off. The third limitation is the ability of the lines connected to the bus to transmit the generated power. A portion of the power generated by renewable sources will be consumed locally by the bus demand. The excess amount will be sent to the network through the bus lines to be used in other buses. The amount of this transmitted power depends on the capacity of the lines. In other words, as much as the capacity of the lines connected to the bus, regardless of the bus voltage limit and power balance, there will be the opportunity to transfer and benefit from the produced renewable energy.

Previous records and history of renewable energy utilization in highly penetrated distribution networks have demonstrated that a percentage of the produced energy is cut off for one or more of the above reasons. This has mainly occurred when renewable energy production is high, or the network load is low. As mentioned above, the curtailment because of power balance can be recovered by a time shift in a produced energy employing a stationary battery energy storage. However, bus overvoltage and feeder overload problem persists. The solution for the renewable curtailment problem is to shift excess produced energy both spatially and temporally, as illustrated in Fig. 1. In this case, the cut off energy is stored and shifted spatially and temporally to be used at another time and location. This spatio-temporal shift can be performed by using a Mobile Battery Energy Storage System (MBES). The MBES is a complete battery system with storage cells, and power converters containerized and mounted a truck [24]. The battery container is permanently mounted on the truck. In other words, it cannot be detached for charging or discharging. This means that movement of the truck without the battery is not possible. The MBES can connect to the network buses for charging, transported to another bus location, and discharge the stored energy. In this way, the unusable produced renewable energy at bus n and time period k is shifted to bus nn and time period kk. Charging, transportation, and discharging of energy is constrained by some technical and economic factors. In the charging state, the MBES has to be connected to one of the network buses. Besides, neither it can power rating of its power converter nor the energy capacity of the storage cells. Similarly, in the discharging state, the MBES has to be attached to one of the network buses and observe power rating and the charge's available state.

There are some different rules for the transportation state. Transporting the MBES between network buses necessitate disconnection from the previous bus, movement to the new location, and finally, connection to the new bus. Performing these actions demand spending a specific time for any specific transportation between network buses. Besides, functioning the MBES imposes some operation costs. The first cost is related to the truck driver, which is a fixed value. The second one is the cost paid for the fuel burnt over transportations. These two cost terms constitute the driving cost of the MBES. Attachment and detachment of the MBES to the grid needs an expert electrical technician. This person has to be contracted based on an options fee and exercise fee paradigm. In this way, the electrical technician receives a fixed daily option fee regardless of the MBES connections and disconnection. Besides, an exercise fee has to be paid for any connection or disconnection of the MBES, which has a predefined daily schedule. These rules and limitation must be mathematically modelled to schedule the MBES optimally. The mathematical formulation for an MBES fleet's optimal operation is proposed in the following regarding the situations mentioned above.

## 3. Mathematical formulation of the proposed model

As discussed earlier, transporting each MBES unit in the network enforces specific situations that have to be met. The MBES transportation governing rules are mathematically formulated one-by-one in the following. Before introducing the proposed optimal MBES, the fleet operation model for renewable curtailment recovery involving sets must be defined. The mathematical model's ultimate goal is to schedule a set of $m$ MBES units in an electric power distribution network with $n$ (or equivalently $nn$) buses over $k$ (or equivalently $kk$) time periods of daily operation horizon. Fig. 2 tabulates the general rules of transporting an MBES unit amongst network buses. Accordingly, a two-dimensional binary variable is used to indicate spatio-temporal status of each MBES unit in the network. This variable, $B^{st}_{(m,n,k)}$, denotes the connection of MBES unit $m$ to bus $n$ of the network at time slice $k$. Obviously, each MBES unit can only connect to one of the network buses at any time slice, formulated in (1). Besides, considering the periodical operation

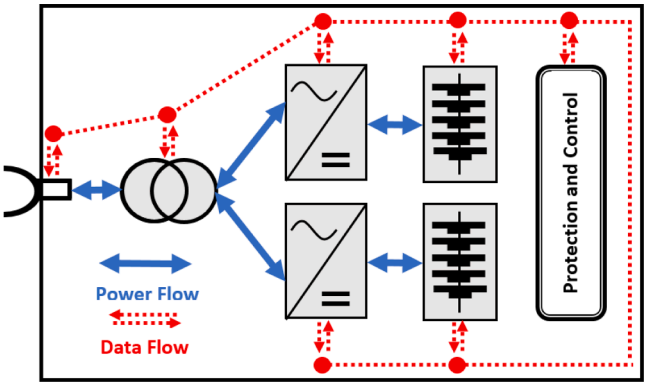


**Fig. 3.** Internal structure of the MCS battery.

paradigm of the distribution, each MBES unit has to be relocated to its initial location before ending the day. This limitation is modelled by (2) where $B^{o}_{(m,n)}$ presents the initial spatio-temporal status

$$\sum_{n} B^{st}_{(m,n,k)} \leq 1 \quad \forall\, m,k \tag{1}$$

$$B^{st}_{(m,n,kk)} = B^{o}_{(m,n)} \quad \forall\, m, kk = K \tag{2}$$

As illustrated by Fig. 2, transporting each MBES unit between network buses necessitates elapsing at a specific time. This time is itself composed of previous bus connection detachment, movement time, and new bus attachment. This Transportation Time (TT) is a constant and predefined value for each movement between network buses, shown by $TT_{(n,nn)}$. This time indicates that the MBES cannot connect to a new bus after disconnecting from the previous one unless disconnected from the network as long as the transmission time between these two. For instance, it supposed that the transportation time between buses 2 and 5 is equal to 2 h in Fig. 3.

This limitation is modelled by (3) and (4). In (3), the value of the spatio-temporal status variable for two non-identical busses cannot be equal to one if the time interval between them is less than the required transportation time. In other words, the time interval between connecting two non-identical buses must be at least equal to the transportation time between them. In (4), the spatio-temporal stats variable is forced to connect to the network after elapsing the required transportation time. It should be noted that there may be some idle (not connected and not transported) statuses for the MBES if (2) is ignored. In Other words, observing (2) ensures that the value of the spatio-temporal binary variable will be equal to zero as long as the transportation time and not any more.

$$B^{st}_{(m,n,k)} + B^{st}_{(m,nn,kk)} \leq 1 \quad \forall\, m,n,nn,k\,, n \neq nn\,,\ kk = \left\{k+1,\ldots,k+TT_{(n,nn)}\right\} \tag{3}$$

$$\sum_{kk=k+1}^{k+TT_{(n,k)}+1} \left[B^{st}_{(m,nn,kk)}\right] \geq B^{st}_{(m,n,k)} \quad \forall\, m,n,nn,k \tag{4}$$

As discussed earlier, transporting and operating each MBES unit in the network imposes specific costs. These costs can be broadly categorized into electrical technician cost and driver (and fuel) cost. Attachment and detachment of the MBES in the network are technical and necessitate a learned person's presence. It should be noted that this human resource is needed only when the MBES is disconnected or connected to the network. In other words, there is no need for the electrical technician when the MBES is static at any network bus or on the road for transportation. As a result, the electrical technician cost can be divided into two parts. The first part is a constant and daily option fee paid regardless of the number of MBES connections and disconnections. The second part is an exercise fee that will be paid based on the number of connections and disconnections. Accordingly, the connections and disconnection of each MBES unit have to be detected. Inequalities (5) and (6) define situations wherein each MBES changes its connection status. In (5), $B^{Co}_{(m,n,k)}$ denotes the establishment of a new bus connection regarding present and previous status. Similarly, $B^{Di}_{(m,n,k)}$ in (6) implies the establishment of a new bus disconnection regarding present and later status.,

$$B^{Co}_{(m,n,k)} \geq B^{st}_{(m,n,k)} - B^{st}_{(m,n,k-1)} \quad \forall\, m,n,k \geq 2 \tag{5}$$

$$B^{Di}_{(m,n,k)} \geq B^{st}_{(m,n,k)} - B^{st}_{(m,n,k+1)} \quad \forall\, m,n,k \leq 23 \tag{6}$$

After defining binary variables indicating connection and disconnection of each MBES unit, the total daily technician cost can be calculated using (7). In this equation, $C^{CT}_{(m)}$, $C^{OF}_{CD}$, and $C^{EF}_{CD}$ denote, in turn, total daily technician cost, technician fixed option fee, and technician exercise fee for each connection or disconnection. The transportation cost can be considered the sum of the truck driver cost and fuel cost. The driver cost is a predefined and fixed daily value independent of the number of transportations. On the contrary, the fuel cost is imposed only when the MBES moves between network buses. The transportation situation can be detected by observing the time periods when the MBES is not connected to the network. In other words, the zero value of spatio-temporal status variable indicates MBEs transportation and fuel consumption. As a result, the inverse of the status binary variables is used to calculate MBES fuel cost and then total driving cost (8). The $C^{DF}_{(m)}$, $C^{DR}_{MB}$, and $C^{FU}_{MB}$ denote total transportation cost of each MBES, fixed daily driver cost, and fuel cost for each driving hour, respectively. The total daily cost of MBES operation can be calculated by summing up (7) and (8).

$$C^{CT}_{(m)} = C^{OF}_{CD} + C^{EF}_{CD} \sum_{(n,k)} \left(B^{Co}_{(n,k)} + B^{Di}_{(n,k)}\right) \quad \forall\, m \tag{7}$$

$$C^{DF}_{(m)} = C^{DR}_{MB} + C^{FU}_{MB} \sum_{(n,k)} \left(1 - B^{St}_{(n,k)}\right) \quad \forall\, m \tag{8}$$

The stored energy in the MBES at any time period ($J^{MB}_{(m,k)}$) has a cumulative nature and depends on the previous periods other than the current one. The present energy exchange, the difference between net charged and discharged volumes, and the previously stored volume constitute current stored energy, as formulated in (9). In this equation, $P^{BC}_{(m,n,k)}$ and $P^{BD}_{(m,n,k)}$ are hourly charging and discharging powers while $\eta^{BC}_{(m)}$ and $\eta^{BD}_{(m)}$ stand for corresponding efficiencies. The relation of the stored energy concerning the nominal energy capacity of the MBES ($E^{MB}_{(m)}$) has to be within permissible State of Charge (SoC) bounds ($SoC^{MB}_{Min}$ and $SoC^{MB}_{Max}$) which is modelled by (10). Like the spatio-temporal status, stored energy in each MBES has to be equal to the initial value after ending the day, denoted by (11).

$$J^{MB}_{(m,k)} = J^{MB}_{(m,k-1)} + \sum_{n} P^{BC}_{(m,n,k)} \eta^{BC}_{(m)} - \sum_{n} \frac{P^{BD}_{(m,n,k)}}{\eta^{BD}_{(m)}} \quad \forall\, m,k \tag{9}$$

$$SoC^{MB}_{Min} \leq \left(J^{MB}_{(m,k)} \Big/ E^{MB}_{(m)}\right) \leq SoC^{MB}_{Max} \quad \forall\, m \tag{10}$$

$$J^{MB}_{(m,k)} = J^{o}_{(m)} \quad \forall\, m, k = K \tag{11}$$

Fig. 3 depicts various part of the whole battery system within the container, including storage cells, power converter(s), and transformer (if needed). As in the figure, there are three limitations on the active and reactive power of the MBES regarding both charging and discharging statuses. The first one is that the MBES can only be charged or discharged at any time period. The second one is that power flowing through it has to be lower than its nominal power [26]. The third one is that the MBES can interact with the network by charging or discharging if connected to a bus. These constraints are modelled for active power

charging and discharging in (12) to (14). Two auxiliary binary variables are used for modelling active power charging ($X^{Ch}_{(m,n,k)}$) and discharging ($X^{Di}_{(m,n,k)}$) status. The inequalities (15) to (17) establish the same limitations on the MBES's inductive ($Qm^{In}_{(m,n,k)}$) and capacitive reactive power ($Qm^{Ca}_{(m,n,k)}$). Similarly, the binary variables $Y^{In}_{(m,n,k)}$ and $Y^{Ca}_{(m,n,k)}$ denote inductive and capacitive reactive power contribution of the MBES, respectively. Also, the $S^{MB}_{(m)}$ denotes power rating for each MBES unit of the network. Beside scalar values of the active and reactive power, the vector of the MBES' apparent power has to be lower than its power rating. This limitation is formulated in (18), where it is handled by piece-wise linearization to keep the total formulation linear [27].

$$X^{Ch}_{(m,n,k)} + X^{Di}_{(m,n,k)} \le B^{st}_{(m,n,k)} \quad \forall m,n,k \tag{12}$$

$$Pm^{Ch}_{(m,n,k)} \le X^{Ch}_{(m,n,k)} S^{MB}_{(m)} \quad \forall m,n,k \tag{13}$$

$$Pm^{Di}_{(m,n,k)} \le X^{Di}_{(m,n,k)} S^{MB}_{(m)} \quad \forall m,n,k \tag{14}$$

$$Y^{In}_{(m,n,k)} + Y^{Ca}_{(m,n,k)} \le B^{st}_{(m,n,k)} \quad \forall m,n,k \tag{15}$$

$$Qm^{In}_{(m,n,k)} \le Y^{In}_{(m,n,k)} S^{MB}_{(m)} \quad \forall m,n,k \tag{16}$$

$$Qm^{Ca}_{(m,n,k)} \le Y^{Ca}_{(m,n,k)} S^{MB}_{(m)} \quad \forall m,n,k \tag{17}$$

$$\left(Pm^{Ch}_{(m,n,k)} + Pm^{Di}_{(m,n,k)}\right)^2 + \left(Qm^{Ch}_{(m,n,k)} + Qm^{Di}_{(m,n,k)}\right)^2 \le \left(S^{MB}_{(m)}\right)^2 \quad \forall m,n,k \tag{18}$$

The cost of the up-stream substation's energy has an incremental nature and increase with the output power growth. Conventionally, a stair-wise function is used to model the substation energy cost function. In this method, the substation's cost of purchasing power is divided into a certain number of price steps, denoted by set $g$. The amount of power supplied by each step is variable ($P^{SS}_{(k,g)}$) and limited by the step size ($\Delta P^{SS}$), as shown by (19). The cost of purchasing power will be calculated with the next step's price by completing each step's power limit. Accordingly, the cost of the total power purchased per hour ($C^{SS}_{(k)}$) is equal to the sum of the product of step price ($\lambda_{(g)}$) in power supplied in that step, as in (20). Similarly, the total power imported per hour ($Po^{Sb}_{(k)}$) is equal to the power purchased on all steps, modelled by (21).

$$P^{SS}_{(k,g)} \le \Delta P^{SS}_{(g)} \quad \forall g,k \tag{19}$$

$$C^{SS}_{(k)} = \sum_g \lambda_{(g)} P^{SS}_{(k,g)} \quad \forall k \tag{20}$$

$$Po^{S}_{(k)} = \sum_g P^{SS}_{(k,g)} \quad \forall k \tag{21}$$

According to the power balance rule, the total active power generated must be equal to the total active power consumption per hour of operation and each network bus. Equalities (22) and (23) present a balance of the active power for the network buses at any time period. The equalities (22) establishes the power balance for the first bus, or equivalently substation bus, of the network. The substation output power is the only real power generator at this bus. The discharging power of the MBES units connected to this bus is treated as a fictitious generator. The summation over discharged power of the MBES units and the substation output power constitute the bus's total injected power. On the contrary, power charging of all MBES units connected to the bus, local bus active power demand ($Pd^{Bs}_{(n,k)}$), and summation over active power flows ($Pf^{Fe}_{(n,nn,k)}$) leaving the bus are bus power consumptions. There is no substation output power in other network buses, but instead, there may be renewable distributed generation resources. The active power balance for these buses is formulated in (23) where $Pg^{Re}_{(r,n,k)}$ denotes maximum power produced by renewable resource $r$ connected to the bus. Besides, $Pc^{Re}_{(r,n,k)}$ presents amount of renewable power curtailed compulsorily. This variable has to be positive and lower than the total renewable power produced in the bus, denoted by (24). The problem aims to maximize renewable power penetration by minimizing these variables' total daily amount, namely imposed curtailment. Similar to the active power, the reactive power balance is established for substation bus and other network buses in (25) and (26). In these equations, $Qo^{Sb}_{(k)}$, $Qd^{Bs}_{(n,k)}$, $Qf^{Fe}_{(n,nn,k)}$ denote reactive power output of the substation, bus local reactive demand, and reactive power low of the lines connected to the bus.

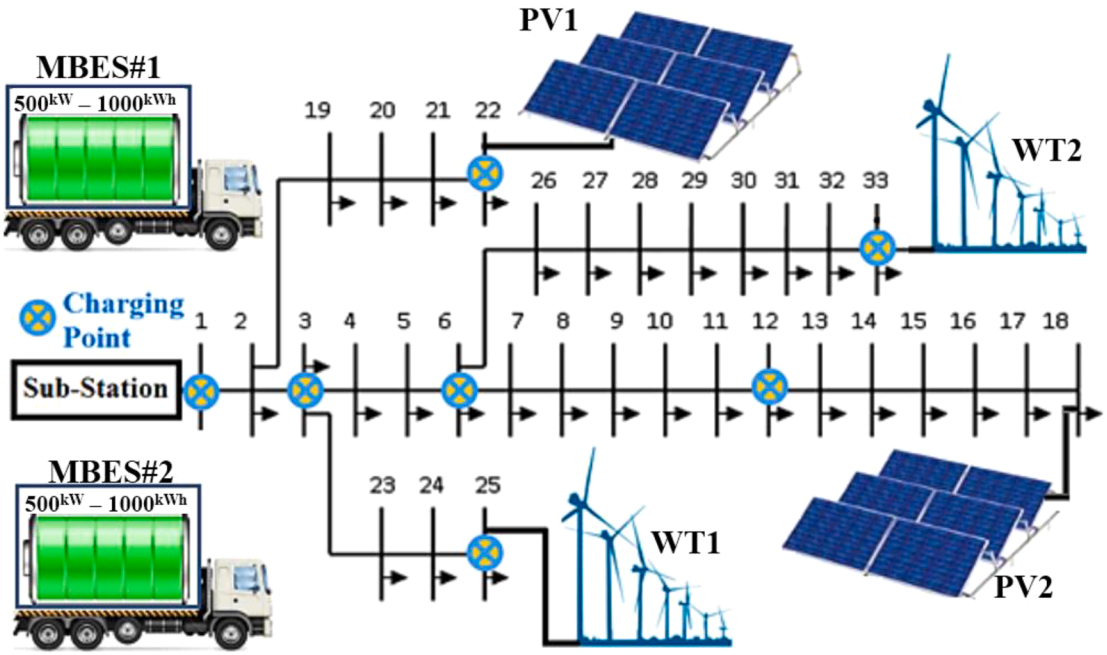


**Fig. 4.** IEEE 33-bus test system with renewable resources and MBES fleet.

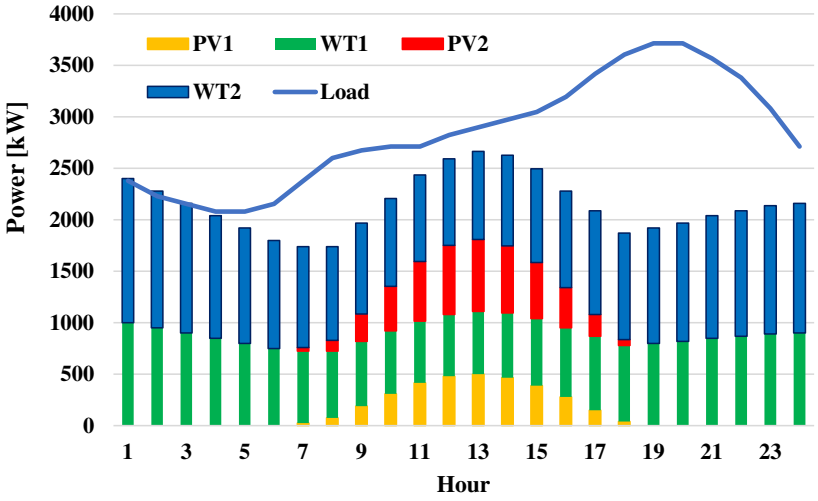


**Fig. 5.** Renewable resources and load profile.

$$Po^{Sb}_{(k)} + \sum_{m} Pm^{Di}_{(m,n,k)} = \sum_{m} Pm^{Ch}_{(m,n,k)} + Pd^{Bs}_{(n,k)} + \sum_{nn} Pf^{Fe}_{(n,nn,k)} \;\forall\, k,\, n = 1 \tag{22}$$

$$\sum_{r}\left(Pg^{Re}_{(r,n,k)} - Pc^{Re}_{(r,n,k)}\right) + \sum_{m} Pm^{Di}_{(m,n,k)} = \sum_{m} Pm^{Ch}_{(m,n,k)} + Pd^{Bs}_{(n,k)} + \sum_{nn} Pf^{Fe}_{(n,nn,k)} \;\forall\, k,\, n \geq 2 \tag{23}$$

$$0 \leq Pc^{Re}_{(r,n,k)} \leq Pg^{Re}_{(r,n,k)} \;\;\forall\, r,\, n, k \tag{24}$$

$$Qo^{Sb}_{(k)} + \sum_{m} Qm^{Ca}_{(m,n,k)} = \sum_{m} Qm^{in}_{(m,n,k)} + Qd^{Bs}_{(n,k)} + \sum_{nn} Qf^{Fe}_{(n,nn,k)} \;\forall\, k,\, n = 1 \tag{25}$$

$$\sum_{m} Qm^{Di}_{(m,n,k)} = \sum_{m} Qm^{Ch}_{(m,n,k)} + Qd^{Bs}_{(n,k)} + \sum_{nn} Qf^{Fe}_{(n,nn,k)} \;\forall\, k,\, n \geq 2 \tag{26}$$

A linear version of the DistFlow equations [28,29] is used to model the relation between bus voltages and line flow, as shown by (27). The line apparent power flow must be lower than its thermal limit, formulated in (28). This non-linear constraint is also handled by piece-wise linearization to maintain the whole model linear. Finally, there is a limitation on the lower and upper bound of the network's bus voltages established in (29).

$$V_{(n,k)} = V_{(nn,k)} - 2\left(R^{Fe}_{(n,nn)} Pf^{Fe}_{(n,nn,k)} + X^{Fe}_{(n,nn)} Qf^{Fe}_{(n,nn,k)}\right) \;\forall n, nn, k \tag{27}$$

$$Pf^{Fe2}_{(n,nn,k)} + Qf^{Fe2}_{(n,nn,k)} \leq \left(S^{Fe}_{(n,nn)}\right)^2 \;\forall n, nn, k \tag{28}$$

$$V^{Bus}_{Min} \leq V_{(n,k)} \leq V^{Bus}_{Max} \;\forall n, k \tag{29}$$

The objective function formulated in (1), i.e., total daily operation cost, comprises summation over substation energy cost along with the MBES fleet operation cost over entire daily operation periods. The substation energy cost is previously calculated in (20). The operation cost of the MBES units, technician (calculated in (7)) and transportation (calculated in (8)), comprises fixed driver cost, fixed technical cost, variable fuel cost, and variable connection and disconnection cost. The problem ultimately aims at lowering total daily operation cost by maximizing renewable energy penetration. This goal can be achieved by MBES fleet employment for curtailment minimization if scheduled optimally.

**Table 1**
Characteristics of MBES units.

| Parameter | Unit | MBES#1 | MBES#2 |
|---|---|---|---|
| **Initial Location** | Bus # | 1 | 6 |
| **Power Rating** | kW | 5000 | |
| **Energy Capacity** | kWh | 1000 | |
| **Lower SoC** | % | 10 | |
| **Upper SoC** | % | 90 | |
| **Initial Energy** | kWh | 100 | |
| **Charging Efficiency** | % | 90 | |
| **Discharging Efficiency** | % | 90 | |
| **Daily Driver Cost** | $ | 25 | |
| **Fuel Cost** | $/h | 5 | |
| **Technician Option Fee** | $ | 20 | |
| **Technician Exercise Fee** | $ | 5 | |

**Table 2**
Transportation time between candidate buses (h).

| Bus | 1 | 3 | 6 | 12 | 22 | 25 | 33 |
|---|---|---|---|---|---|---|---|
| **1** | 0 | 1 | 2 | 3 | 2 | 2 | 3 |
| **3** | 1 | 0 | 1 | 2 | 1 | 1 | 2 |
| **6** | 2 | 1 | 0 | 1 | 2 | 2 | 1 |
| **12** | 3 | 2 | 1 | 0 | 3 | 3 | 2 |
| **22** | 2 | 1 | 2 | 3 | 0 | 2 | 3 |
| **25** | 2 | 1 | 2 | 3 | 2 | 0 | 3 |
| **33** | 3 | 2 | 1 | 2 | 3 | | 0 |

$$Min \quad CO^{Tot} = \sum_{k} C^{SS}_{(k)} + \sum_{m}\left(C^{CT}_{(m)} + C^{DF}_{(m)}\right) \tag{30}$$

## 4. Numerical test, inputs, and parameters

The model proposed and explained previously is texted on a sample system in this section. The IEEE 33-bus standard test system is used as the studied distribution network. The line and load data are presented in [30]. The system is equipped with additional renewable power sources in the form of PV panels and wind turbines, as depicted in Fig. 4.

As the figure shows, The PV panels are installed in buses 18 and 22 while wind turbines are connected to buses 25 and 33. Hourly power production of these renewable resources, along with the load demand, is depicted in Fig. 5. As in the figure, the PV2 and WT2 distributed resources have larger capacities than PV1 and WT1, respectively. Besides, the figure denotes a small over-generation of renewable-based power at

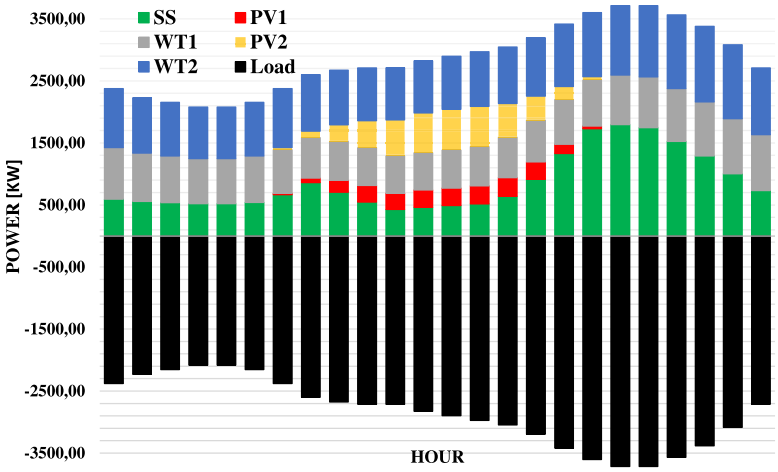


**Fig. 6.** Hourly power balance for CODN case.

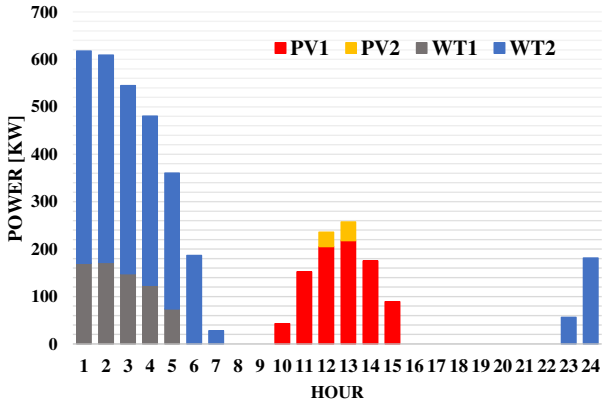


**Fig. 7.** Breakdown of hourly curtailed renewable energy for CODN case.

the early hours of the day. The MBES fleet comprises two truck-mounted containerized battery energy storage systems with a 500 kW power rating and 1000 kWh energy capacity. The charging and discharging efficiency is both equal to 0.9. It is supposed that the MBESs can connect to buses 1, 3, 6, 12, 22, 25, and 33, considering parking limitations and connection requirements. Technical and cost data related to the MBES fleet are presented in Table 1. Besides, Table 2 presents the transportation time between candidate buses. The pie-wise linear substation cost is as [23].

The bus voltage magnitude variation is limited to 5% to simulate the renewable curtailment's real-life situation. Besides, the capacity of the line connecting WT1 wind farm lateral to the main feeder, namely line 6–26, is confined to 500 kVA while the capacity of the other lines is equal to 3000 kVA. The two different cases are simulated to compare and analyse the effectiveness of the MBES fleet operation. The first one is the conventional distribution network without an MBES fleet, titled CODN. The second one is the network equipped with the MBES fleet, denoted by MFDN. The mathematical model is implemented in GAMS 32 software [31] and solved using the CPLEX 20 solver [32]. In the following, first, the results for the former case are presented. Then, the effect of MBES fleet operation is analysed, and the results are compared. Finally, the optimal spatio-temporal and power-energy schedule of each MBES, causing the latter case results are presented.

## 5. Conventional distribution network without MBES (CODN)

Fig. 5 demonstrates the hourly power balance for the considered distribution network without the MEBS fleet. As indicated previously in the modelling section, the hourly load demand is supplied from the renewable distributed generation resources and the up-stream substation. Fig. 5 denotes a high share of the wind farms in the load supply considering the higher and 24-hour power production range. In contrast, the PV panels' power contributes to load supply only during non-hours when solar radiation is abundant. Besides, the power production share of the PV2 is higher than the PV1 plant. The critical point is that the substation injects the power at all time periods of operation and follows the load demand.

**Table 3**
Total daily results for both cases.

| Item | CODN | MFDN | Difference | |
|---|---|---|---|---|
| | | | Net | % |
| **Substation Energy Cost ($)** | 3456 | 2845 | −611 | −17.68 |
| **MBES Operation Cost ($)** | – | 170 | +170 | +100 |
| **Total Operation Cost ($)** | 3456 | 3015 | −441 | −12.77 |
| **Used Renewable (kWh)** | 47,608 | 50,170 | +2562 | +5.38 |
| **Curtailed Renewable (kWh)** | 4016 | 1454 | −2562 | −63.79 |
| **Substation Energy (kWh)** | 20,673 | 18,545 | 2128 | −10.29 |
| **MBES energy Losses (kWh)** | – | 434 | +487 | +100 |

By comparing Figs. 6 with 5, the status of total renewable-based power generation concerning the load demand, some critical points can be deduced. The first one is that the difference between total renewable power generation with the load demand in Fig. 5 should be supplied from the substation. This value is much lower than the substation output power resulting from the simulation in Fig. 6. Another point is that total renewable power generation exceeds or equals load demand at the day's initial hours, meaning zero substation output power. However, the hourly power output of the substation in Fig. 6 violates this deduction. The reason is behind the curtailed renewable energy. Fig. 7 depicts the hourly curtailed renewable energy for various resources. As in the figure, there is a considerable volume of curtailment in the produced renewable energy, especially for WT2 and PV1 resources. The reason for this considerable power cut is excess power generation at the early hours of the morning, bus voltage violation (overvoltage), and feeder overload. The technical limitation of the network resulting in enforced renewable cut off has caused importing power from the up-stream substation despite abundant internal power generation. The bus installation location and the production time of the renewable resources shape the usable and curtailed renewable energy share. The substation supplies 20,673 kWh from the total 68,281 kWh demanded energy. Total energy from renewable resources is equal to 51,624 kWh. From this value, 47,608 kWh is used, and the remaining

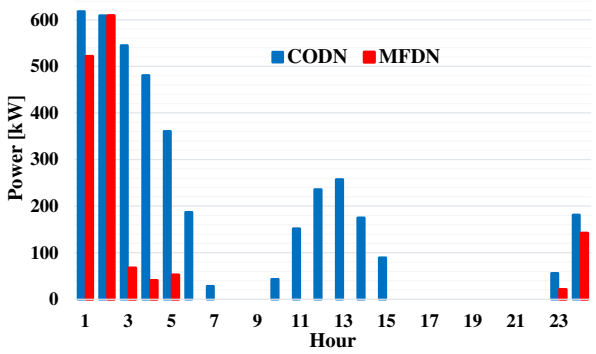


**Fig. 8.** Total hourly curtailed renewable energy for both cases.

4016 kWh is curtailed. The total curtailed renewable energy can reduce about 20% of energy imported from the substation if recovered. The proposed model's application to achieve this goal utilizing the MBES fleet is described in the following.

## 6. Effect of MBES fleet operation (MFDN) and comparison

Table 3 presents the total daily results of the simulations for both cases and the absolute and relative differences. As it can be observed, total injected energy by the substation is reduced by 2128 kWh, equal to 10.29%. This reduction in imported energy has reduced the total daily energy cost by 611 $ or equivalently 17.68%. The point to be noted here is that the substation energy cost reduction percentage is much more than the corresponding energy reduction. The reason is behind the incremental energy cost and value of price arbitrage performed by the MBES fleet.

In other words, the results show that a reduction in the substation output power has occurred mainly at peak load demand with higher energy prices. Operating the MBES fleet costs 170 $ because of the driver cost, fuel cost, technician exercise and option fee. As a result, the total daily operation cost is reduced by 12.77%. This reduction is achieved by recovering curtailed renewable energy. The optimal MBES fleet operation helps recover 2562 kWh out of the total 4016 daily curtailed renewable energy, meaning a net 63.79 reduction. This reduction in the curtailed energy denotes a 5.38 growth, given the total used renewable energy. It should be noted that a total value of 434 kWh of the absorbed energy by the MBES fleet is wasted as the internal losses. Fig. 8 demonstrates total hourly curtailed energy for both cases. The figure magnifies the critical role of the MBES fleet in curtailment reduction. The point to be noted here is that total curtailed renewable energy is still high at the early hours of the day, and the MBES fleet has not been able to reduce it. There are two reasons for this problem with the same origin. The first one is the hourly power generated more than the load demand, and the second one is the bus upper cottage limit violation. These

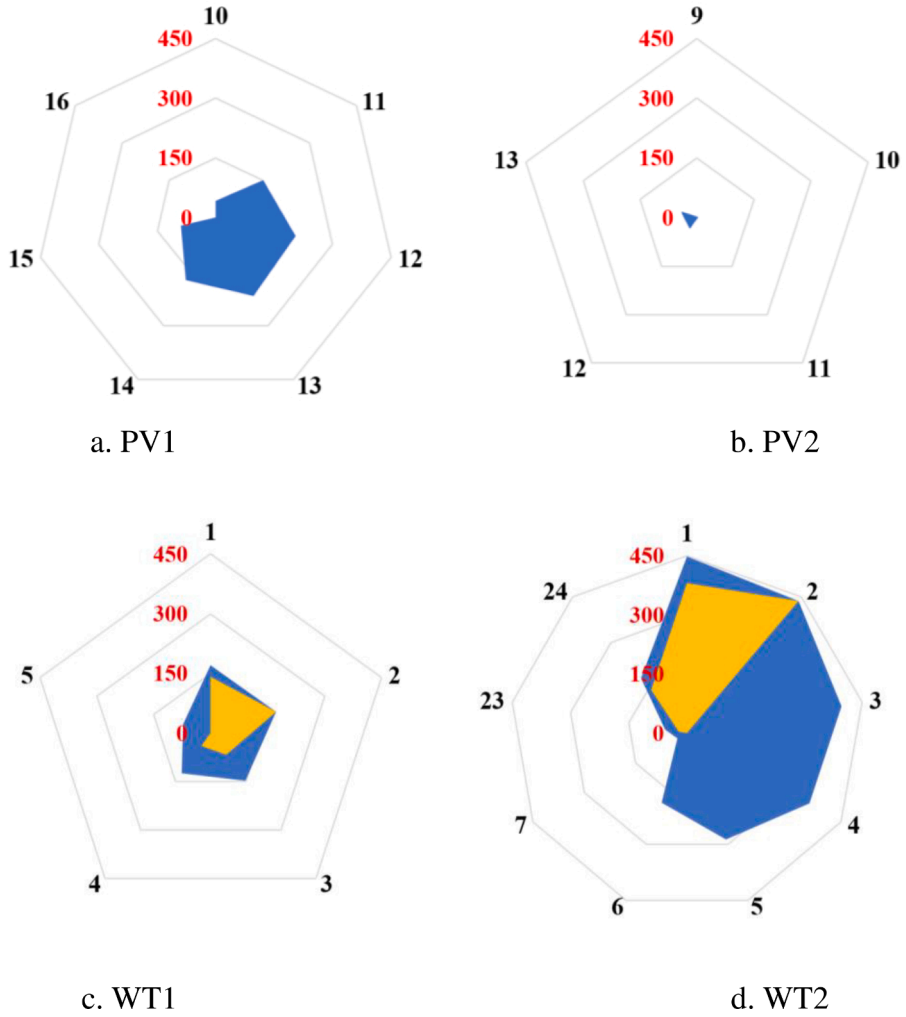


**Fig. 9.** Hourly curtailed renewable energy by source (Blue = CODN, Yellow = MFDN). (For interpretation of the references to colour in this figure legend, the reader is referred to the web version of this article.)

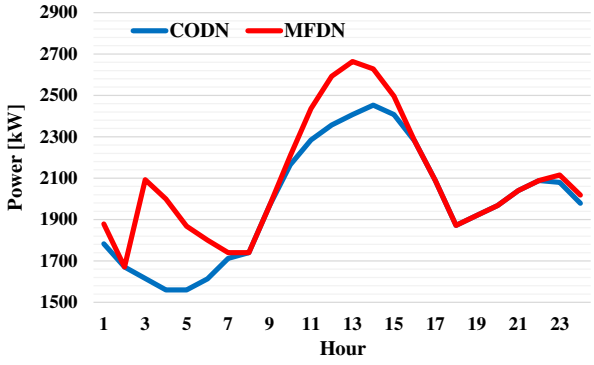


**Fig. 10.** Total hourly used renewable energy for both cases.

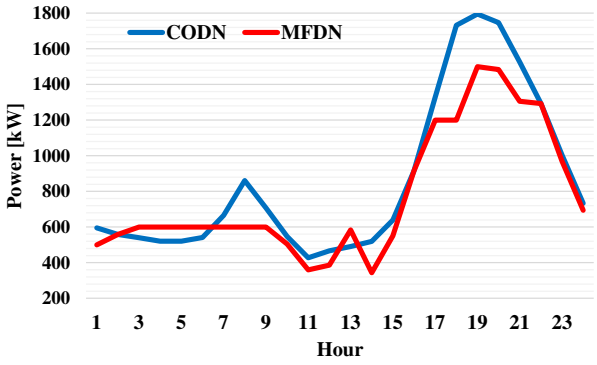


**Fig. 11.** Hourly output power of substation for both cases.

consequences result from the low load demand on the one hand and high renewable potential by wind turbines on the other hand.

Fig. 9 shows the breakdown of hourly curtailed renewable energy by the renewable plant for both cases. As in the table, the MBES fleet has recovered curtailed energy for both PV plants completely. However, a portion of the curtailed renewable energy produced by both wind farms is remained due to the high share. Accordingly, the distributed resource WT1 has benefited from the MBES fleet less than other resources with 38.5 recovered energy. The WT2, which is the largest distributed resource of the network, has constituted the highest share of the curtailed renewable energy in both cases. The MBES fleet has reduced curtailed energy for this resource by 50.60%.

Recovering curtailed renewable energy or equivalently increasing used renewable energy will result in lower power import from the upstream substation in turn. Fig. 10 displays the total hourly used renewable energy for both cases. As it can be observed, the MBES fleet has increased used renewable energy by recovering the curtailed portion at two periods, hours 2–7 and 11–15. Fig. 11 exhibits the hourly output power of the substation for both cases. As in the figure, the reliance on the substation power has increased using the MBES fleet at two periods in accordance with the renewable energy curtailment mitigation. In other words, by comparing Figs. 10 and Fig. 11, one can conclude that the absorbed curtailed renewable energy is used to supply a portion of the load demand at later periods. Accordingly, the substation output power's first and second peak periods during hours 7–10 and 17–22 is reduced, utilizing energy previously stored in the batteries. This reduction in the substation outpour power will increase its loading and connected feeders in turn. Besides, there will be an additional capacity to cover more load growth in the future.

**Table 4**
MBES fleet transportation statistics and cost.

| Item | | | MBES#1 | MBES#2 |
|---|---|---|---|---|
| # of Transports | | | 3 | 2 |
| Bus Connections | | | 1, 3, 22 | 6, 33 |
| # of Connections | | | 3 | 2 |
| # of Disconnections | | | 3 | 2 |
| Trans. Cost ($) | Driver | | 25 | 25 |
| | Fuel | | 20 | 10 |
| | Technician | Option Fee | 20 | 20 |
| | | Exercise Fee | 30 | 20 |
| | | Total | 50 | 40 |
| | Total | | 95 | 75 |

## 7. MBES fleet spatio-temporal and power-energy schedule

The benefits mentioned above is achieved via optimal scheduling of the MBES fleet described in this section. The scheduling denotes determining optimal hourly spatio-temporal status along with the charge-discharge power of each MBES. Table 4 presents a summary of the statistics related to mobile battery units. As in the table, MBES#1 experiences three transportations while MBES#2 transports only two times. Besides, MBES#1 changes the connection between buses 1, 3, and 22. On the contrary, MBES#2 moves only between buses 6 and 33. According to the required transportations, MBES#1 and MBES#2 need three connections/disconnections. The table also presents the detail of the transportation cost for each mobile battery unit. Accordingly, the transportation cost of MBES#1 with a higher number of movements is more than MBES#2.

Fig. 12 displays the hourly spatio-temporal status of the MBES units. As it can be observed, each MBES unit covers a part of the network in terms of energy recovery. Accordingly, the PV1 renewable plant is handled by MBES#1. To lower renewable curtailment in this distributed resource, MBES#1 moves between its initial location, namely bus 1 and buses 3 and 22. As in the figure, MBES#1 has left its initial location immediately after initiating operation periods by moving to bus 3. After spending 4 h in bus 3, it moves again to the new location in bus 22. MBES#1 has been 9 h at bus 22 and then leaves it to be at its initial location. The MBES# unit has tried to recover WT1 energy curtailment by transportation to bus 33. Accordingly, it moves to be at bus 33 for charging during hours 3–7 and then returns to its initial location at hour 9.

At last, Fig. 13 depicts hourly power and energy scheduling for each MBES. As can be observed, the mobile batteries' power and energy schedule are in accordance with their spatio-temporal status, namely Fig. 12. As a result, MBES#1 starts power charging from hour 3 when it arrived at bus 3. Similarly, MBES#2 had absorbed curtailed renewable energy from hour 3 when it arrived at bus 33. The first period of power charging for both mobile batteries takes about 4 h. At this time, the stored energy for MBES#1 has reached its allowable value, 900 kWh, while MBES#2 has used 800 kWh of the storage capacity. A portion of the stored energy in both MBES units is released during hours 7–10 to handle the load profile's first peak. The energy deficit is compensated at the second power charging period during hours 11–13. The MBES#1 changes its location while the MBES#2 stays at the previous bus. At this time, both MBES#1 has ultimately charged. The curtailed energy stored is discharged from hours 17 to 21 to cope with the second and main peak demand. Finally, stored energy in both mobile batteries reaches its minimum allowable value, i.e., 100 kWh.

## 8. Conclusions

Mitigating a portion of the curtailed energy will increase the renewable resources' penetration level without capacity enhancement. The recovered cut off energy can improve the distribution networks' economic, technical, and environmental performance by decreasing

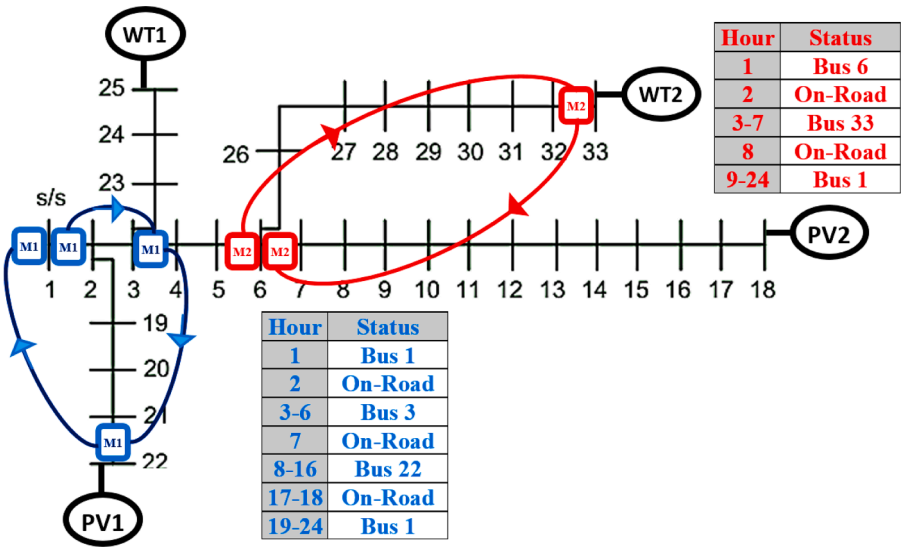


| Hour | Status |
|---|---|
| 1 | Bus 6 |
| 2 | On-Road |
| 3-7 | Bus 33 |
| 8 | On-Road |
| 9-24 | Bus 1 |

| Hour | Status |
|---|---|
| 1 | Bus 1 |
| 2 | On-Road |
| 3-6 | Bus 3 |
| 7 | On-Road |
| 8-16 | Bus 22 |
| 17-18 | On-Road |
| 19-24 | Bus 1 |

**Fig. 12.** MBES fleet transportation schedule (Blue=MBES#1 and Red=MBES#2).

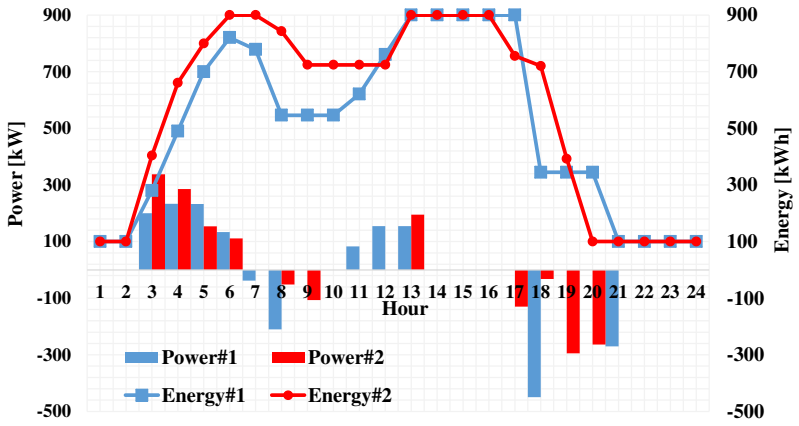


**Fig. 13.** Hourly power and energy for each MBES.

reliance on distribution network supply. The MBES systems can store and recover a considerable share of the curtailed energy owing to their variable spatial and temporal production nature. Accordingly, a new scheduling model was proposed in this paper to benefit from a fleet of the MBES units for curtailment mitigation. The proposed model, while linear, considers MEBS' transportation time and cost, efficiently and by new formulations. The simulation results demonstrate a 12.77% reduction in the total daily operation cost utilizing the MBES fleet. This cost reduction is achieved as a result of a 63.79% recovery in the curtailed renewable energy employing two MBES units. Besides, the spatio-temporal and power-energy status of the MBES units is highly dependent on the time and location of renewable resources with abundant curtailed energy. As a future work, the operation model of the separable mobile battery storage system can be addressed. In this case, the battery container can be detached from the truck and one truck can be used for transporting multiple battery containers.

## CRediT authorship contribution statement

**Hedayat Saboori:** Conceptualization, Methodology, Software, Validation, Formal analysis, Resources, Data curation, Writing – original draft, Visualization. **Shahram Jadid:** Conceptualization, Investigation, Writing – review & editing, Supervision, Project administration.

## Declaration of Competing Interest

The authors hereby confirm no conflict of interest and financial/personal interest or belief that could affect the paper's objectivity. In addition, the authors have not received any funding or research grants in the course of study, research or assembly of the manuscript.

## References

[1] I. Dincer, Renewable energy and sustainable development: a crucial review, Renew. Sustain. Energy Rev. 4 (2) (2000) 157–175.
[2] R. Hemmati, H. Saboori, Emergence of hybrid energy storage systems in renewable energy and transport applications–A review, Renew. Sustain. Energy Rev. 65 (2016) 11–23.
[3] B.V. Mathiesen, H. Lund, K. Karlsson, 100% Renewable energy systems, climate mitigation and economic growth, Appl. Energy 88 (2) (2011) 488–501.
[4] L. Bird, et al., Wind and solar energy curtailment: a review of international experience, Renew. Sustain. Energy Rev. 65 (2016) 577–586.
[5] P. Liu, P. Chu, Wind power and photovoltaic power: how to improve the accommodation capability of renewable electricity generation in China? Int. J. Energy Res. 42 (7) (2018) 2320–2343.
[6] Q. Zhou, J.W. Bialek, Generation curtailment to manage voltage constraints in distribution networks, IET Generat., Trans. Dis.. 1 (3) (2007) 492–498.
[7] C. Li, et al., Comprehensive review of renewable energy curtailment and avoidance: a specific example in China, Renew. Sustain. Energy Rev. 41 (2015) 1067–1079.
[8] R. Golden, B. Paulos, Curtailment of renewable energy in California and beyond, Electr. J. 28 (6) (2015) 36–50.

[9] J.C. Koj, C. Wulf, P. Zapp, Environmental impacts of power-to-X systems-A review of technological and methodological choices in Life Cycle Assessments, Renew. Sustain. Energy Rev. 112 (2019) 865–879.
[10] L. Ju, et al., A risk aversion optimal model for microenergy grid low carbon-oriented operation considering power-to-gas and gas storage tank, Int. J. Energy Res. 43 (10) (2019) 5506–5525.
[11] Gu, C., et al. "Assessing operational benefits of large-scale energy storage in power system: comprehensive framework, quantitative analysis, and decoupling method." Int. J. Energy Res.
[12] H. Saboori, et al., Energy storage planning in electric power distribution networks–A state-of-the-art review, Renew. Sustain. Energy Rev. 79 (2017) 1108–1121.
[13] A. Naderipour, et al., Sustainable and reliable hybrid AC/DC microgrid planning considering technology choice of equipment, Sustain. Energy, Grids Netw. 23 (2020), 100386.
[14] Y. Deng, et al., Operational planning of centralized charging stations utilizing second-life battery energy storage systems, IEEE Trans. Sustain. Energy 12 (1) (2020) 387–399.
[15] Y. Zhang, et al., Optimal whole-life-cycle planning of battery energy storage for multi-functional services in power systems, IEEE Trans. Sustain. Energy 11 (4) (2019) 2077–2086.
[16] H. Saboori, S. Jadid, Mobile and self-powered battery energy storage system in distribution networks–Modeling, operation optimization, and comparison with stationary counterpart, J. Energy Storage 42 (2021), 103068.
[17] Y. Zheng, et al., Optimal integration of mobile battery energy storage in distribution system with renewables, J. Modern Power Syst. Clean Energy 3 (4) (2015) 589–596.
[18] J. Kim, Y. Dvorkin, Enhancing distribution system resilience with mobile energy storage and microgrids, IEEE Trans. Smart Grid. 10 (5) (2018) 4996–5006.
[19] S. Lei, et al., Routing and scheduling of mobile power sources for distribution system resilience enhancement, IEEE Trans. Smart Grid 10 (5) (2018) 5650–5662.
[20] S. Yao, et al., Rolling optimization of mobile energy storage fleets for resilient service restoration, IEEE Trans. Smart Grid 11 (2) (2019) 1030–1043.
[21] S. Yao, P. Wang, T. Zhao, Transportable energy storage for more resilient distribution systems with multiple microgrids, IEEE Trans. Smart Grid 10 (3) (2018) 3331–3341.
[22] F. Mohamad, J. Teh, C.-M. Lai, Optimum allocation of battery energy storage systems for power grid enhanced with solar energy, Energy 223 (2021), 120105.
[23] C.-M. Lai, J. Teh, Network topology optimisation based on dynamic thermal rating and battery storage systems for improved wind penetration and reliability, Appl. Energy 305 (2022), 117837.
[24] J. Teh, C.-M. Lai, Reliability impacts of the dynamic thermal rating and battery energy storage systems on wind-integrated power networks, Sustain. Energy, Grids Netw. 20 (2019), 100268.
[25] M.K. Metwaly, J. Teh, Probabilistic peak demand matching by battery energy storage alongside dynamic thermal ratings and demand response for enhanced network reliability, IEEE Access 8 (2020) 181547–181559 [25]Transportable Energy Storage Systems Project. EPRI, Palo Alto, CA 2009. 1017818.
[26] H. Mehrjerdi, R. Hemmati, Modeling and optimal scheduling of battery energy storage systems in electric power distribution networks, J. Clean. Prod. 234 (2019) 810–821.
[27] H. Mehrjerdi, Simultaneous load leveling and voltage profile improvement in distribution networks by optimal battery storage planning, Energy 181 (2019) 916–926.
[28] G.Y. Yang, et al., TCSC allocation based on line flow based equations via mixed-integer programming, IEEE Trans. Power Syst. 22 (4) (2007) 2262–2269.
[29] M. Farivar, S.H. Low, Branch flow model: relaxations and convexification—Part I, IEEE Trans. Power Syst. 28 (3) (2013) 2554–2564.
[30] M.E. Baran, F.F. Wu, Network reconfiguration in distribution systems for loss reduction and load balancing, IEEE Power Eng. Rev. 9 (4) (1989) 101–102.
[31] A. Brook, D. Kendrick, A. Meeraus, GAMS, a user's guide, ACM Signum. Newslett. 23 (3–4) (1988) 10–11.
[32] I.L.O.G Cplex, 11.0 User's Manual, ILOG SA, Gentilly, France, 2007, p. 32.